

# Fatigue Crack Paths in Shafts Subjected to Bending and Torsion

T. Lassen<sup>1</sup> and A. Spagnoli<sup>2</sup>

<sup>1</sup> University of Stavanger, Norway – tom.lassen@uis.no

<sup>2</sup> University of Parma, Italy – spagnoli@unipr.it

**ABSTRACT.** *In the present article an in-service fatigue failure of a large propeller shaft is analyzed and discussed. Observed crack growth path and fatigue life are compared with fracture mechanics calculations for various loading modes to determine the most likely fatigue damage mechanism. It was found that the fatigue crack leading to failure of the shaft emanated from a flaw on the surface. The initial flaw had a depth in the range of 0.5-1.0 mm. The subsequent crack shapes were revealed from crack front beach marks. Larger cracks had approximately a semi-elliptical shape with an average aspect ratio near 0.8. Although the design stresses in the shaft were fluctuating shear stresses due to torsion, unforeseen rotating bending stresses may have occurred due to misalignment of the shaft bearings. Based on the observation of the crack front shapes, it was shown that the fatigue failure of the shaft was driven by a multiaxial stress situation dominated by rotating bending stresses at an early stage.*

## INTRODUCTION

One of the intermediate steel propeller shafts onboard on a shuttle tanker failed due to fatigue crack growth. The fracture occurred after 20 months of service time only. The fracture appeared on the plain cylindrical part of the shaft and not in the vicinity of any geometrical stress raiser. When such in-service failures occur, the failure investigation is often characterized by two challenges. The first challenge is the lack of information, the second challenge is the need for fast and correct decision to prevent failures of similar shafts still running. To tackle the situation, a thorough examination of the design criteria, service condition and damage appearance has to be carried out. Then, failure hypotheses have to be proposed and rejected based on available evidence. In the present case it was obviously a fatigue failure, but the dominant loading mode and stress level were not known. Linear Elastic Fracture Mechanics (LEFM) was used in conjunction with Paris law to determine the evolution of the crack. To carry out the necessary calculations of the Stress Intensity Factor (SIF), the size of the initial crack and the crack shape evolution during propagation have to be known. Based on the given fatigue life and on inspection of the fatigue fracture surface, a detailed study was carried out to determine the crack growth path and corresponding most likely loading mode.

The examination of the shaft revealed a pre-existing flaw in the surface with a depth

in the range of 0.5 to 1.0 mm. Even with the presence of this crack-like defect, the fatigue failure cannot be explained by the design fluctuating shear stresses, since these stresses are benign with a stress range less than 10 MPa. A more likely hypothesis was that the shaft had been subjected to rotating bending stresses, unintentionally introduced by the misalignment of the shaft bearings. A detailed examination of the shape of the crack front marks on the fatigue fracture surface was carried out. These beach marks are rest lines occurring during service periods with low fluctuating stresses. The shapes were assessed and compared to semi-elliptical and circular shapes that are likely to appear under various loading modes. From a theoretical point of view, crack fronts will grow towards a shape where every point along the crack front has the same SIF. This iso-SIF shape is depending on crack depth and is different for different loading modes. By comparing with the shapes actually appearing on the failed fracture surface, some loading modes can be rejected, whereas others can be more likely. There are two criteria that should be fulfilled for the most likely loading mode and stress range level: the crack shape evolution should be similar to observation made on the failed shaft; the fatigue life calculated by fracture mechanics should coincide with the experienced time to failure.

Based on these two criteria a fracture mechanics model that fits the facts given from the examination of the failed shaft was established. The results from the analysis were added to other important information. One of the shaft bearings was replaced during the first service year due to indication of high temperature. The event may support the bearing misalignment hypothesis. Furthermore, stress measurements carried out on similar shafts after the failure did not reveal any other stress levels than the design shear stress range of 10 MPa. This makes the failed shaft a special case, and the aim of the present study is to pin point the peculiarities that caused the failure. The scope of work is both theoretical and practical. It is demonstrated how detailed fracture mechanics modelling can reveal the dominant loading mode and stress level [1]. Practical preventive measures to avoid similar failures are discussed and recommended [2].

## **DESCRIPTION OF FAILURE**

The fracture occurred in the intermediate part, between bearing and flange, of the propeller shaft in the shuttle tanker. The crack had started from a flaw on the surface of the shaft. The fatigue fracture surface was characterized by its smooth appearance with almost no plastic strain. As is shown in Fig. 1, beach marks, indicating the position of the crack front at various stages during propagation, have a typical semi-elliptical shape. The final rupture was ductile with a crack size close to 250 mm. This is about 70% of the shaft diameter  $D$  ( $D = 360$  mm).

The geometry of five chosen crack fronts was studied in detail, see Fig. 2. Each crack front is designated by a number and for crack no 2-5 the associated label has its bottom left hand corner located where the actual crack front intersects with the free surface of the shaft. The shape data of the cracks according to the notation of Fig. 3a are given in Table 1. The smallest crack designated no 1 is difficult to trace and the geometry is

somewhat uncertain. It has a smaller aspect ratio than the others and is most likely formed by the coalescence of two circular shaped cracks. All the other cracks are semi-elliptical with a rather high aspect ratio  $a/b$ . It can also be seen from Fig. 2 that all the crack fronts have an intersection angle with the free surface close to  $90^\circ$ . The fatigue fracture plane is normal to the shaft axis for cracks no 1 and 2. After the crack depth passes 9.2 mm (crack no 2,  $a/2R=0.026$ ,  $a/b=0.75$ ) the fatigue fracture plane shifts towards an angle of  $60^\circ$  with respect to the shaft axis. The parameter  $\alpha$  listed in Table 1 will be defined in the ensuing text related to Fig. 3b.



Figure 1 - Fatigue fracture surface and final fracture.

Table 1 - Crack shape of the failed shaft

Crack no	$A/2R$	$a/2h$	$a/b$	$\alpha$
1	0.015	-	-	-
2	0.026	0.38	0.75	0.06
3	0.07	0.46	0.89	0.04
4	0.10	0.39	0.76	0.13
5	0.25	0.45	0.82	0.17

## FATIGUE CRACK GROWTH MODELING

### *Crack Growth and Possible Loading Modes*

A shaft may be subjected to cyclic stresses due to three possible loading modes: axial loading, bending loading and torsion [3,4]. For the shaft under consideration all three loading modes are possible, although only the torsional loading mode was foreseen at the design stage. When a crack is present in the shaft, fracture mode I might occur due to axial or bending loading, and fracture modes II (shearing) and III (tearing) might occur due to torsion. A mixed fracture mode is possible when the shaft is subjected to a combination of the loading modes. However, during propagation of large cracks, fracture mode I is often dominating.

It is well established that a fatigue crack tends to initiate at the plane of maximal shear stress due to a slip band mechanism (stage 1, mode II). Afterwards the crack

propagates in a plane perpendicular to the maximal applied principal stress range (stage 2, mode I). In the present case where initial flaws exist, the stage 1 can be neglected so that, if the shaft is subjected to axial or bending loading, the entire crack growth will be in a plane perpendicular to the shaft axis under mode I.

The present shaft has a crack plane perpendicular to the shaft axis from the start up to a crack depth of approximately 9 mm. After this crack depth is passed, the crack plane orientation changes to 60° with respect to the shaft axis. Hence, it is likely that the main driving force for the fatigue growth in the early stage has been rotating bending.

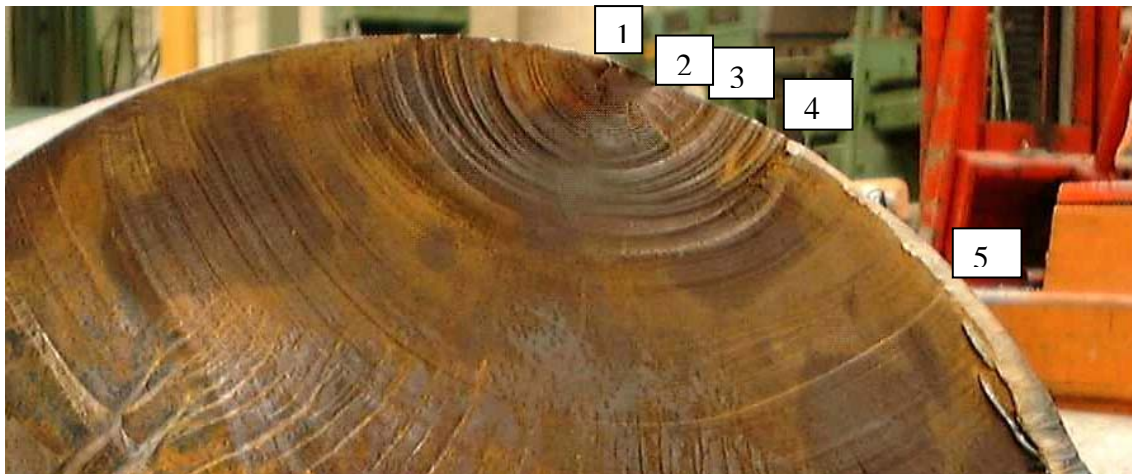


Figure 2 - Chosen crack fronts for shape definition.

### ***Description of Crack Front Shape and SIF***

For a given cracked component in order to determine the dimensionless SIF  $F = K/(\sigma\sqrt{\pi a})$ , the crack geometry must have a clear definition. Carpinteri [3] defined an elliptical-arc surface crack in a round bar, as it is shown in Fig. 3a. It is assumed that the shape of the crack front is part of an elliptical arc with half minor axis equal to the crack depth and with half major axis measured along the tangent at the shaft surface. The length of the two half-axes is denoted by  $a$  and  $b$  respectively. The SIF can be calculated at any point along the crack front but we are particularly interested in the deepest point A and the surface point B. In Fig. 3a, a general ellipse with half-axes  $a$  and  $b$  together with two special cases is shown. These cases are a straight fronted and a semi-circular crack.

Levan and Royer [4] chose to describe the surface crack front as a circular arc with a constant radius  $R'$ , see Fig. 3b where the two special cases from Fig. 3a are recognized. The intermediate crack geometries between these two limit cases are defined by a shape parameter  $\alpha = B_0B/B_0B_1$  ( $\alpha=0$  is for the semi-circular crack and  $\alpha=1$  for the straight fronted crack).

It can be seen that for the cracks no 3 to 5 identified in Fig. 2 the departure of the front from a circle even for the worst case of crack no 4 is not striking and one may

conclude that both the above mentioned semi-elliptical and the circular approaches are applicable.

Based on the work of Carpinteri [3] and Levan and Royer [4], the values of the dimensionless SIF  $F$  are given in Table 2 for axial and bending loading respectively. The values pertaining to  $a/2R > 0$  are taken from Carpinteri, whereas the values for the limit case of  $a/2R = 0$  are taken from Levan and Royer. As the two references have slightly different definition of crack shape the results are not directly comparable. It has been assumed that  $\alpha = 0.1$  is equal to  $a/b = 0.8$  for all practical purposes, although the first crack front is a part of a circular arc and the second is a semi-elliptical crack. The discrepancy between the SIF values from the two references was found to be within 7%.

As can be seen from the table, regardless of the loading mode, a straight fronted crack always has the highest SIF at the deepest point A and, hence, it tends to grow towards a more curved shape. For a semi-circular crack the surface point B has the highest SIF. Hence this crack tends to grow towards a less curved shape, particularly under bending loading. Levan and Royer [4] argued that the shape of a fatigue crack would follow an iso-SIF curve under axial and bending loading. The values of the parameter  $\alpha$ , corresponding to iso-SIF crack fronts for axial and bending loading, are reported in Table 3.

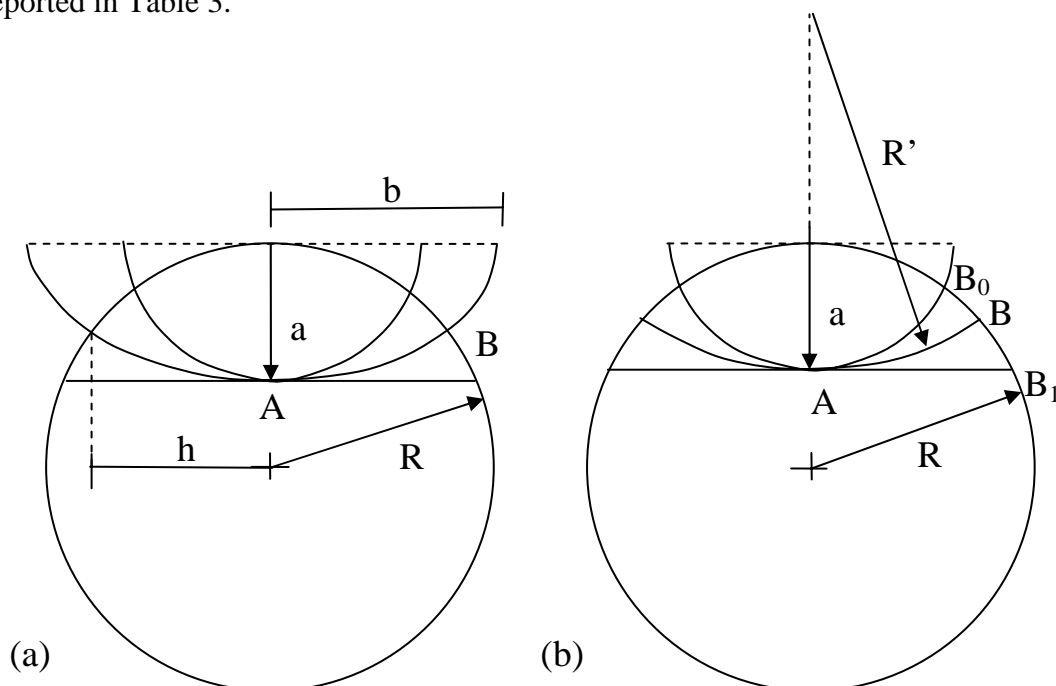


Figure 3 – (a) Crack front shape modelled as a semi-ellipse [3]; (b) Crack front shape modelled as a part of a circle [4].

As can be seen, crack under bending loading will tend to have a more straight fronted shape (higher  $\alpha$ ) than cracks subjected to axial loading. By comparison with the measurements in Table 1, it is not possible to decide the actual loading mode from the crack front shapes. Crack no 2 in Table 1 with  $a/2R = 0.026$  has  $\alpha = 0.06$  which is closest

to bending loading in Table 3. Crack no 4 in Table 1 with  $a/2R=0.10$  has  $\alpha = 0.13$  which is far to low compared to the values of axial or bending loading in Table 3. Crack no 3 shows again a departure from the iso-SIF criterion. The only possible conclusion is that bending loading is likely up to crack no 2. The more circular shapes of larger cracks can be related to the fact that torsion becomes relatively more important after that stage. According to [3] the crack front shape tends to stabilize during fatigue propagation to  $a/b=0.78$  for both axial and bending loading. This is in very good accordance with the measured values in Table 1 up to crack no 2.

Table 2 – Dimensionless SIF  $F$  for axial and bending loading

a/b	Point	a/2R							
		0.0		0.1		0.2		0.3	
		Axial	Bend.	Axial	Bend.	Axial	Bend.	Axial	Bend.
0 ( $\alpha=1$ )	A	1.12	1.12	1.05	0.86	1.23	0.87	1.49	0.89
	B	0.58	0.58	0.78	0.63	0.93	0.61	1.19	0.65
0.8 ( $\alpha \approx 0.1$ )	A	0.80	0.78	0.79	0.64	0.93	0.63	1.07	0.62
	B	0.61	0.63	0.72	0.64	0.90	0.72	1.13	0.77
1.0 ( $\alpha=0$ )	A	0.66	0.66	0.71	0.58	0.82	0.55	0.93	0.56
	B	0.65	0.65	0.71	0.63	0.86	0.69	1.03	0.82

Table 3 - Typical values of the parameter  $\alpha$  for iso-SIF crack fronts under axial and bending loading

a/2R	Axial loading	Bending loading
0.02	0.03	0.04
0.12	0.14	0.29
0.3	0.42	0.59

## FATIGUE LIFE ESTIMATION FOR THE FAILED SHAFT

At the design stage of the shaft under consideration, only the torsional loading and the corresponding shear stresses were analysed. However, rotating bending stresses due to misalignment of the shaft bearings may have occurred during the first part of the service life. Based on the examination of the fatigue fracture surface it seems appropriate to divide the crack growth in the following two phases.

Phase 1 is defined by the crack growth from the initial crack depth ( $a=0.5$  mm) to the crack depth related to crack no 2 ( $a=9.2$  mm). It is assumed that this phase is totally dominated by rotating bending stresses. The shear stresses are below the threshold value in this crack growth phase. The assumption is supported by the fact that the crack plane is perpendicular to the shaft axis and that the semi-elliptical shape of crack no 2 is defined by  $a/b=0.7$ , i.e. close to that of an iso-SIF curve for bending loading. This phase consumes most of the experienced fatigue life.

Phase 2 is a mixed mode crack growth dominated by rotating bending stresses but with the torsional shear stresses playing a role. Such a mixed mode crack growth might

give a shift in the orientation of the crack plane [5], since the direction of the maximum principal stress is not parallel to the shaft axis. This can explain the 60° angle between the fatigue crack surface and the shaft axis after the crack has passed the crack no 2. This phase is theoretically interesting but represents a minor part of the experienced fatigue life in the present case.

During Phase 1, it is assumed that fatigue crack growth is governed by the Paris law ( $da/dN = C(\Delta K)^m$ , where  $da/dN$  is the crack growth rate and  $C$  and  $m$  are material crack growth parameters). In order to calculate the number of cycles needed for the crack to propagate from an initial crack depth to a final crack depth, the Paris law must be integrated between the two crack depths.

The shaft is made of steel quality 42CrMo4 with a carbon content of 0.42% and Cr and Mo content of 1% and 0.25 % respectively. The yield stress is equal to 700 MPa and the ultimate tensile stress to 800 MPa. The material crack growth parameters for this specific steel are not known. In the lack of specific data the recommended values from BS7910 [6] are chosen:  $m = 3.0$ ;  $C = 4.9 \times 10^{-12}$ .

As a first approach, by integrating the Paris law between  $a_i=0.5$  mm and  $a_f=90$  mm ( $a_f$  is equal to 25% of the shaft diameter) and equating the result to the experienced fatigue life of 20 months, we work out an effective stress range due to rotating bending. Therefore such a range causes the same damage as the real time-dependent stress history. If we assume a shaft rotation of 127 rpm (corresponding to a loading frequency of 2.1 Hz) we have approximately  $1.1 \times 10^8$  cycles in the experienced fatigue life of 20 months and, hence, the effective stress range results to be  $\Delta\sigma=49$  MPa. As can be observed from the crack growth history in Fig. 4, the 85% of the fatigue lifetime is spent before reaching a crack depth of 10 mm.

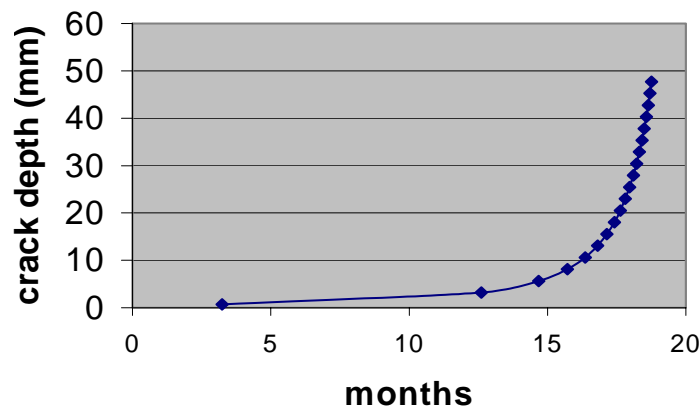


Figure 4 - Crack growth history for  $a_i=0.5$  mm and  $\Delta\sigma=49$  MPa.

## CONCLUSIONS

1) The shaft failed due to fatigue crack growth. The crack emanated from a flaw at the surface of the shaft. This crack-like defect had a depth close to 0.5 mm. The initial flaw was probably introduced during fabrication or by a weld arc strike during maintenance.

2) Crack shape definitions based on semi-elliptical or circular shaped fronts are both applicable to describe real fatigue crack geometries occurring during service. The iso-SIF criterion for crack shape growth seems to be valid for small cracks. Larger cracks follow a path where their shape is closer to a semi-circular one.

3) Based on both observed crack path and fatigue life, unintentional rotating bending is considered to be the driving force for the crack growth. The rotating bending may have occurred due to bearing misalignment. As a matter of fact, the design fluctuating torsional stresses are by far too low to inflict the observed rapid fatigue crack propagation, as has been verified by a fatigue threshold assessment.

5) It is very likely that the combination of a surface flaw and the presence of rotating bending is a peculiar case for the failed shaft.

6) To prevent fatigue failure in propeller shafts there are some general safeguards that are recommended. It should be verified that the resonance condition of torsional vibration in the shaft is avoided. Furthermore, measures should be taken during maintenance work to avoid introduction of surface flaws, either caused by weld arc strikes or sharp tools. The entire surface should be protected.

7) The easiest and most economical strategy to reveal any danger of fatigue failure is to carry out in-service stress measurements in the shafts in order to verify whether they are subjected to high rotating bending stresses. Crack inspection is a more cumbersome task to carry out due to the fact that the cracks do not necessarily appear at local notches but anywhere on the large surface. Furthermore, the cracks have a hidden path before the acceleration sets in. Only in cases where high stresses are revealed, inspection should be carried out.

## REFERENCES

1. Schijve, J. (2001) *Fatigue of Structures and Materials*, Kluwer Academic Publisher.
2. DNV Publication (2001) *Casualty Information: Failure of intermediate shafts*, DNV Publication no. 3/01.
3. Carpinteri, A. (1992) *Fatigue Fract. Engng Mater Struct.* **15**, 365-376.
4. Levan, A., Royer, J. (1993) *Int. J. Fracture* **61**, 71-99.
5. Lassen, T., Recho, N. (2006). In: *International Scientific and Technical Encyclopedia*, Chapter 11: Mixed Mode Loading.
6. BS7910 (2005) *Guide on methods for assessing the acceptability of flaws in metallic structures*, BSI.